Passage through a barrier with a slowly increasing control parameter

C. Nicolis
Institut Royal Météorologique de Belgique, Avenue Circulaire 3, 1180 Brussels, Belgium

G. Nicolis
Center for Nonlinear Phenomena and Complex Systems, Université Libre de Bruxelles, Code Postal 231, Boulevard du Triomphe, 1050 Brussels, Belgium

(Received 1 March 2000)

A bistable system subjected to noise and a slow increase of the parameter controlling the instability is studied, with emphasis on the kinetics of the transitions across the barrier separating the stable states. It is shown that the presence of a ramp in the control parameter may considerably affect the distribution of probability mass on the two sides of the barrier as compared to the predictions of the classical Kramers theory.

PACS number(s): 05.40.−a, 05.10.Gg

I. INTRODUCTION

Transitions between simultaneously stable states separated by a barrier and induced by intrinsic fluctuations or by external noise are one of the most representative problems at the interface of nonlinear science and stochastic processes. They arise in a wide variety of contexts, from electronic circuits to chemical kinetics, earth sciences, and biology [1,2].

Ordinarily, following Kramers's pioneering contribution [3], the problem is mapped onto a Langevin equation with a nonlinear deterministic part and additive white noise or, equivalently, onto a diffusion process governed by a Fokker-Planck equation with nonlinear drift and constant diffusion coefficient. In the simplest setting of a single variable x admitting in the noiseless limit two stable solutions separated by an intermediate unstable one, these equations read

$$\frac{dx}{dt}=\lambda x-x^3+F(t), \tag{1a}$$

$$\langle F(t)\rangle=0,\langle F(t)F(t')\rangle=q^2\delta(t-t') \tag{1b}$$

(Langevin equation),

and

$$\frac{\partial p}{\partial x}=-\frac{\partial}{\partial x}(\lambda x-x^3)p+\frac{q^2}{2}\frac{\partial^2 p}{\partial x^2}, \tag{2}$$

(Fokker-Planck equation).

In writing Eqs. (1) and (2) we used the generic form of supercritical pitchfork bifurcation [4], for which a single control parameter λ is sufficient to unfold the full set of possible behaviors. A different situation pertains to hysteresis for which a second control parameter, accounting for the effect of an imperfection in the above generic form, is necessary. Although the analysis reported in this paper carries through in this case as well, in what follows we shall focus on problems in which the noiseless (deterministic) dynamics is amenable to a supercritical pitchfork bifurcation.

As is well known, in the absence of noise and for $\lambda>0$ the dynamics generated by Eqs. (1) and (2) gives rise to three invariant sets: the unstable fixed point $x_0=0$, and the two basins of attraction $(-\infty, 0)$ and $(0, \infty)$ of, respectively, the fixed points $x_-=-\lambda^{1/2}$ and $x_+=\lambda^{1/2}$. In the presence of noise this invariance is abolished, and one observes transitions between the two basins. In the limit in which the noise is weak and the two deterministic stable states are well separated, these transitions occur on a characteristic time scale given by the Kramers formula

$$\tau_\pm\approx\pi[-U''(x_0)U''(x_\pm)]^{-1/2}\exp\left[\frac{2}{q^2}\Delta U_\pm\right], \tag{3}$$

where $U(x)$ is the kinetic potential

$$U(x)=-\lambda\frac{x^2}{2}+\frac{x^4}{4} \tag{4a}$$

and $\Delta U_\pm$ the potential barrier

$$\Delta U_\pm=U(x_0)-U(x_\pm)=\frac{\lambda^2}{4}. \tag{4b}$$

The conditions of the validity of these results are summarized by the inequality $\Delta U_\pm \gg q^2/2$.

Typically, in the above studies, the control parameter λ is held fixed during the evolution of the variable x. Now, in many real world situations this is unrealistic in view of the variability and complexity of the environment in which a given system is embedded. In particular, it may happen that λ describes the effect of a constraint that is gradually switched on during the evolution of the variable x, a situation usually referred to as a *ramp*,

$$\lambda=\lambda_0+\varepsilon t, \quad \varepsilon\ll 1. \tag{5}$$

The effect of such ramps on the deterministic dynamics has been the subject of several investigations in the context of nonlinear optics [5] and reaction-diffusion systems [6]. The influence of noise on the dynamics around the unstable point $x_0=0$ has also been analyzed [7–9]. In the present study we

report results concerned with the full, nonlinear system—Eqs. (1) and (2) in the presence of both noise and a ramp in the form of Eq. (5)—with emphasis on the kinetics of transitions across the barrier.

In Sec. II the principal effects of the ramp on the deterministic dynamics are compiled. The stochastic dynamics in the presence of the ramp is formulated in Sec. III. The analytic results obtained are evaluated in Sec. IV and compared with the results of the direct numerical solution of the Langevin and Fokker-Planck equations. The main conclusions are summarized in Sec. V.

II. DETERMINISTIC DYNAMICS IN THE PRESENCE OF A RAMP

In this section we are concerned with a dynamical system described by the evolution equation

$$\frac{dx}{dt}=(\lambda_0+\varepsilon t)x-x^3. \tag{6}$$

The exact solution of this equation is

$$x(t)=\exp\left(\lambda_0 t+\varepsilon\frac{t^2}{2}\right)\times\frac{x_0}{\left\{1+2x_0^2\int_0^t d\tau\exp\left[2\left(\lambda_0\tau+\varepsilon\frac{\tau^2}{2}\right)\right]\right\}^{1/2}}. \tag{7}$$

Its dependence on t, λ_0, and ε is not very transparent. Interesting information may nevertheless be obtained by applying the Hölder inequality,

$$\int_0^t d\tau f^\alpha g^\beta\leqslant\left(\int_0^t d\tau f\right)^\alpha\left(\int_0^t d\tau g\right)^\beta.$$

Setting $\alpha=\beta=\frac{1}{2}$, $f=\exp\{2[\lambda_0\tau+\varepsilon(\tau^2/2)]\}$, $g=1$, and taking the limit of long times one obtains

$$x(t)\leqslant(\varepsilon t)^{1/2}\frac{1}{\int_0^{\varepsilon^{1/2}t}d\xi\exp\left[-\frac{\lambda_0}{\varepsilon^{1/2}}(\varepsilon^{1/2}t-\xi)-\frac{1}{2}(\varepsilon t^2-\xi^2)\right]}. \tag{8}$$

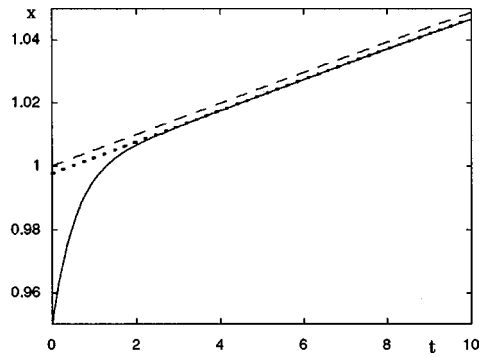

FIG. 1. Time dependence of x for initial conditions $x(0)<\lambda_0^{1/2}$. Dominant part of solution $x^{(0)}$, Eq. (10) (dashed line); numerical solution of Eq. (6) with $x(0)=\lambda_0^{1/2}-\epsilon(1/4\lambda_0^{3/2})$ (dotted line) and $x(0)=0.95$ (full line). Parameter values $\lambda_0=1$, $\epsilon=0.01$.

Since the integral in the denominator converges rapidly to some limiting value, Eq. (8) shows that $x(t)$ is bounded for long times by $C_\varepsilon(\varepsilon t)^{1/2}$, where C_ε is a (generally ϵ dependent) constant.

To arrive at a sharper result and to also study the transients prior to this long time evolution, we now seek perturbative solutions of Eq. (6). Two situations need to be envisaged, depending on the initial conditions.

A. Initial conditions near $x_\pm=\pm\sqrt{\lambda_0}$

Let us set $\tau=\lambda_0+\varepsilon t$, with $\lambda_0>0$. Equation (6) becomes

$$\varepsilon\frac{dx}{d\tau}=\tau x-x^3. \tag{9}$$

We seek solutions of the form

$$x=x^{(0)}+\varepsilon x^{(1)}+\cdots. \tag{10}$$

Substituting into Eq. (6) and identifying equal powers of ε one obtains (for concreteness we limit ourselves, without loss of generality, to states starting near x_+)

$$x^{(0)}=\tau^{1/2}=(\lambda_0+\varepsilon t)^{1/2},\qquad x^{(1)}=-\frac{1}{4\tau^{3/2}}=-\frac{1}{4(\lambda_0+\varepsilon t)^{3/2}}. \tag{11}$$

Notice that $x^{(0)}$ cancels the right hand side of Eq. (9). We shall therefore refer from now on to this part as the *adiabatic approximation.*

Expansion (10) limits us to initial conditions less than $\lambda_0^{1/2}$. Figure 1 depicts the t dependence of the dominant part $x^{(0)}$ of the analytic solution (dashed line) along with the result of the integration of Eq. (6) with a typical initial condition $x(0)<\lambda_0^{1/2}$ (full lines) and an initial condition (dots) matching expansion (10). The agreement is very satisfactory except for a short initial layer for the case of unmatched initial conditions. This layer depends very weakly on ϵ and is essentially determined by the value of λ_0.

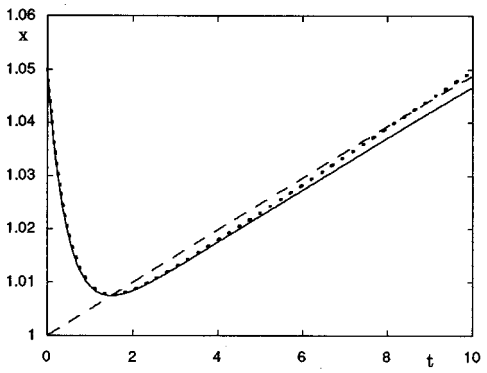

FIG. 2. As in Fig. 1 but for initial conditions $x(0)>\lambda_0$. Dominant part of the solution $x^{(0)}$ (dashed line); exact solution of the linearized equation (12) for the excess variable z with $x=z+\lambda_0^{1/2}$ (dotted line); and numerical solution of Eq. (6) (full line). Initial condition $x(0)=1.05$.

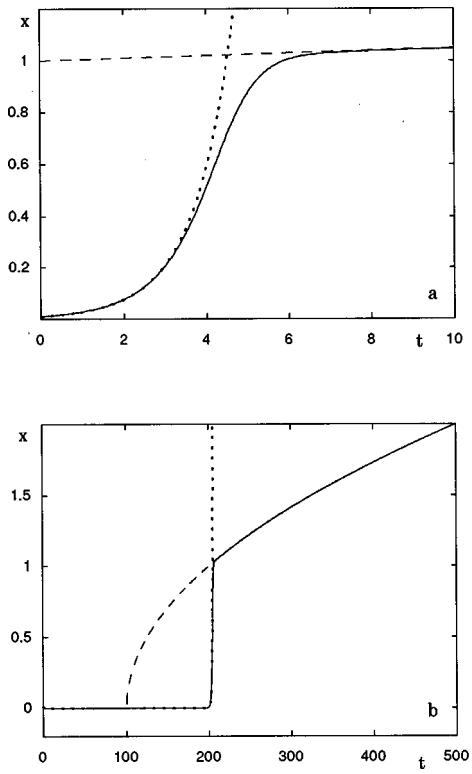

FIG. 3. As in Fig. 1 but for initial conditions $x(0)$ close to zero. Dominant part of solution, $x^{(0)}$ (dashed line); solution of the linearized equation (14) (dotted line); and numerical solution of Eq. (6) (full line) with $x(0)=0.01$. Parameter values $\lambda_0=1$ (a), $\lambda_0=-1$ (b).

To treat initial conditions slightly larger than $\lambda_0^{1/2}$ it is convenient to express Eq. (6) in terms of the excess variable $z=x-\lambda_0^{1/2}$. One obtains

$$\frac{dz}{dt}=\varepsilon\lambda_0^{1/2}t+(\varepsilon t-2\lambda_0)z-3\lambda_0^{1/2}z^2-z^3. \tag{12}$$

We notice that in this representation the ramp is no longer purely multiplicative as in Eq. (6), but gives rise to an additive contribution as well.

Starting with z positive but close to zero, owing to the stability of the ''ghost'' state $z=0$ in the limit $\varepsilon\to 0$, one expects for short times a tendency to decrease from this initial state, in order to reach $z=0$ (or $x=\lambda_0^{1/2}$). Sooner or later, however, this transient crosses over with the dominant part of the perturbative solution $x^{(0)}$, and follows thereafter the same type of evolution as in Fig. 1. The dynamics prior to the crossover can be analyzed from the linearized part of Eq. (12), whose exact solution is easily found to be

$$z^{(0)}=\exp\left(\frac{\tau^2}{2\varepsilon}\right)\exp\left(-\frac{2\lambda_0^2}{\varepsilon}\right)\left\{z(0)+\sqrt{\frac{\pi}{2\varepsilon}}\left[\operatorname{erf}\left(\frac{\tau}{\sqrt{2\varepsilon}}\right)-\operatorname{erf}\left(-\frac{2\lambda_0}{\sqrt{2\varepsilon}}\right)\right]-\lambda_0^{1/2}\left[\exp\left(-\frac{\tau^2}{2\varepsilon}\right)-\exp\left(\frac{2\lambda_0^2}{\varepsilon}\right)\right]\right\}, \tag{13a}$$

with

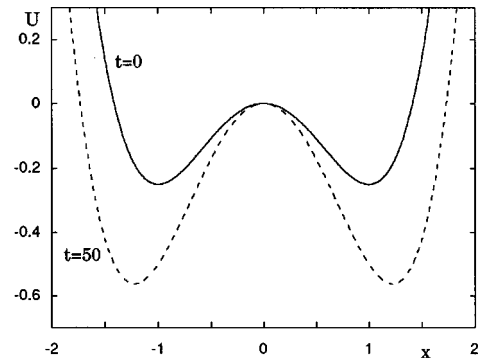

FIG. 4. Snapshots of the potential $U(x,t)$ corresponding to Eq. (6). Parameter values as in Fig. 1.

$$\tau=\varepsilon t-2\lambda_0. \tag{13b}$$

In Fig. 2 this solution (dots) is depicted, along with the result of the integration of Eq. (6), with the same initial condition (full line) and the dominant part of the perturbative expansion $x^{(0)}$ (dashed line). The evolution is in full agreement with the previously drawn qualitative picture. The crossover time is essentially the time it takes to reach the minimum. For a given initial condition it diminishes (weakly) as ϵ is increased. We do not further address the extension of the perturbative approach itself to match the initial condition, as this type of problem has been analyzed in depth in Ref. [5].

B. Initial conditions near $x_0=0$

Consider for concreteness, and without loss of generality, a positive initial condition. For $\lambda_0>0$, owing to the instability of the ghost state $x_0=0$ in the limit $\varepsilon\to 0$, one expects as before, for short times, a tendency to evolve toward $\lambda_0^{1/2}$, which will entail in the present case an increase of the initial value of x. This initial tendency can be determined from the linearized version of Eq. (6), whose solution reads

$$x(t)=x(0)\exp\left[\left(\lambda_0 t+\frac{\varepsilon t^2}{2}\right)\right]. \tag{14}$$

Eventually this transient will cross over with $x^{(0)}$ and follow thereafter the characteristic square-root-in-t evolution of Fig. 1. The crossover time t^* can be estimated by the relation

$$(\lambda_0+\varepsilon t^*)^{1/2}\approx x(0)\exp\left[\left(\lambda_0 t^*+\varepsilon\frac{t^{*2}}{2}\right)\right]. \tag{15}$$

In Fig. 3(a) the early time evolution given by Eq. (14) is plotted in dots along with the numerical solution of the full nonlinear equation (6) (full lines) and $x^{(0)}$ (dashed lines). The results corroborate the above qualitative picture, including the estimate of the crossover time, Eq. (15).

Figure 3(b) depicts the result of the numerical integration of Eq. (6) for $\lambda_0<0$ (full line) along with those of Eq. (14) (dots) and $x^{(0)}$ (dashed lines). The unexpected feature is the extra delay, first discovered by Erneux and Mandel [5], during which the system stays in the vicinity of $x_0=0$ before jumping, superexponentially, toward $x^{(0)}$. The delay time corresponds to the time necessary to build a positive expo-

nent in Eq. (14), and is thus given by $t_d \approx 2|\lambda_0|/\varepsilon$. The crossover time t^* is still given by Eq. (15), the difference $t^* - t_d$ being the duration of the jump.

III. STOCHASTIC DYNAMICS IN THE PRESENCE OF A RAMP

We come now to the main objective of our study, namely, to analyze the dynamics of the fluctuations in the presence of the ramp [Eq. (5)]. This amounts to augmenting Eq. (6) with a noise term subject to conditions (1b),

$$\frac{dx}{dt} = -\frac{\partial U(x,t)}{\partial x} + F(t), \tag{16}$$

where $U(x,t)$ is the extended form of the kinetic potential accounting for the ramp

$$U(x,t) = -(\lambda_0 + \varepsilon t)\frac{x^2}{2} + \frac{x^4}{4}. \tag{17}$$

The probability density $p(x,t)$ satisfies then the augmented Fokker-Planck equation

$$\frac{\partial p}{\partial t} = -\frac{\partial}{\partial x}[(\lambda_0 + \varepsilon t)x - x^3]p + \frac{q^2}{2}\frac{\partial^2 p}{\partial x^2}. \tag{18}$$

An elegant analysis of the various stages of the transient behavior of the probability density $p(x,t)$ in the absence of ramp has been developed by Suzuki [10]. Rather than try to extend Suzuki's approach when a ramp is introduced, we here limit the scope of our study to the long time regime in which the only relevant process is the transfer of probability mass across the potential barrier.

We first study the structure of the potential $U(x,t)$. We still have three extrema, just as in the case $\varepsilon = 0$ [Eq. (4a)], two of which depend now on t:

$$\begin{aligned} x_0 &= 0, \\ x_\pm &= \pm\sqrt{\lambda_0 + \varepsilon t}. \end{aligned} \tag{19a}$$

Notice that $x_\pm$ is just the part $x^{(0)}$ of the solution of the deterministic equation referred to in Sec. 2 as the adiabatic approximation.

The corresponding values of the potential are

$$\begin{aligned} U(0) &= 0, \\ U_\pm(t) &= -\tfrac{1}{4}(\lambda_0 + \varepsilon t)^2, \end{aligned} \tag{19b}$$

leading to a potential barrier

$$\Delta U_\pm(t) = \tfrac{1}{4}(\lambda_0 + \varepsilon t)^2. \tag{19c}$$

Figure 4 depicts two snapshots of $U(x,t)$ for $t = 0$ and $t > 0$. We observe that as time grows the minima move away from $x_0 = 0$ and become, at the same time, deeper. If the noise strength q^2 is reasonably small one may therefore expect that in the regime of long times and in the spirit of Kramers's approach [Eqs. (3) and (4)], $p(x,t)$ will essentially be given by two local Gaussians centered on $x_\pm(t)$, whose weights $N_\pm(t)$ will be slowly varying as a result of the transitions across the barrier. We are thus led to the stochastic version of the adiabatic approximation [1,11],

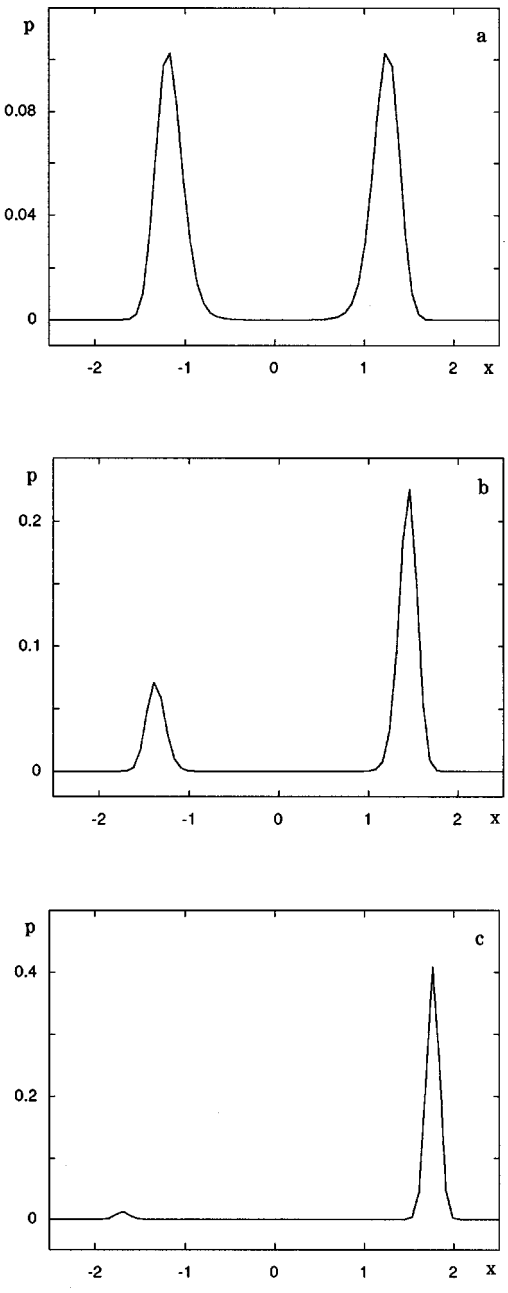

FIG. 5. Probability distribution in the limit of long times obtained numerically from Eq. (18) with $\lambda_0 = 1$, $\epsilon = 10^{-4}$, and $q^2 = 0.12$ (a); $q^2 = 0.08$ (b); and $q^2 = 0.06$ (c).

$$p(x,t) = N_-(t)\phi_-(x,t) + N_+(t)\phi_+(x,t). \tag{20a}$$

The form of $\phi_\pm$ is obtained by expanding $U(x,t)$ around $x_\pm$, keeping only the first nontrivial (here quadratic) term,

$$\phi_\pm = \sqrt{\frac{2(\lambda_0 + \varepsilon t)}{\pi q^2}}\exp\left[-\frac{2(\lambda_0 + \varepsilon t)\{x - [\pm(\lambda_0 + \varepsilon t)]\}^2}{q^2}\right], \tag{20b}$$

showing that, as time goes on, $\phi_\pm$ becomes increasingly narrower around its extremum $\pm(\lambda_0 + \varepsilon t)$.

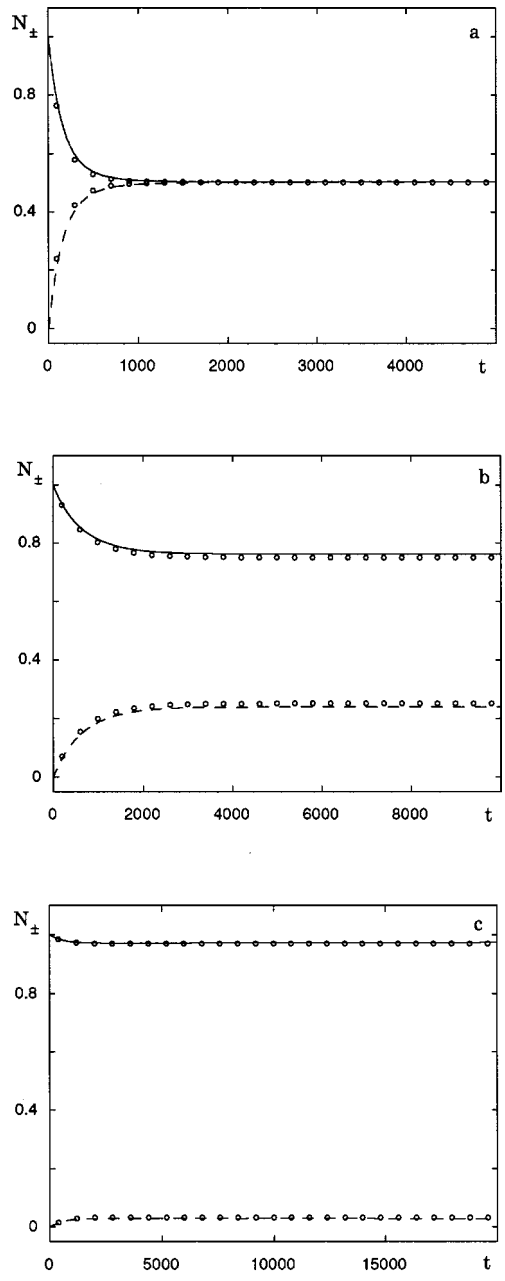

FIG. 6. Time evolution of the probability masses around the two basins N_+ (full line) and N_- (dashed line) as obtained numerically from Eq. (18) with initial condition $N_+(0)=1$, $N_-(0)=0$. Empty circles correspond to the analytical result, Eq. (24). Parameter values as in Fig. 5.

We turn next to the dynamics of the weights $N_\pm(t)$, which carry the interesting information concerning the transitions across the barrier. In order to disentangle the transient behavior from an initial state favoring x_+ or x_-, from the equipartition case in which the two quasiattraction basins are given the same probability mass and hence there is no further evolution, we set

$$N_\pm(t)=\tfrac{1}{2}\pm\delta N(t). \tag{21}$$

The excess probability mass $\delta N(t)$ obeys then, in the adiabatic approximation to which our study is limited, the rate equation [1,11]

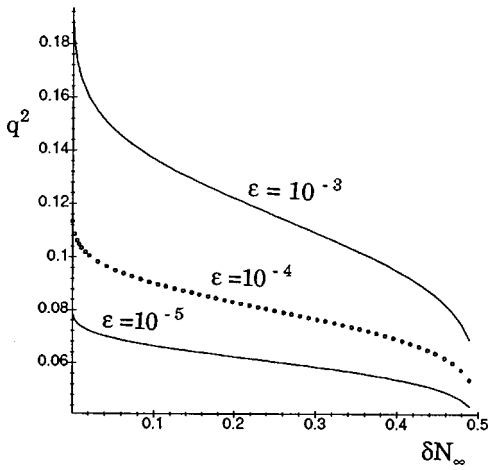

FIG. 7. Sensitivity of the asymptotic value of the excess probability mass δN_∞ on the noise strength q^2 and on the rate of the ramp ϵ as obtained from Eq. (25). Parameter values $\lambda_0=1$ and an initial probability distribution peaked on one basin, $\delta N(0)=0.5$.

$$\frac{d\delta N}{dt}=-\frac{1}{\tau(t)}\,\delta N, \tag{22}$$

where $\tau(t)$ is formally given by Eq. (3), in which U, ΔU now account for the presence of the ramp. Combining this with Eqs. (19), one thus gets

$$\tau^{-1}(t)\approx\frac{\sqrt{2}}{\pi}(\lambda_0+\varepsilon t)e^{-[(\lambda_0+\varepsilon t)^2/2q^2]}. \tag{23}$$

Equation (22), when subject to expression (23) for τ, can be integrated exactly, yielding

$$\delta N(t)=\delta N(0)\exp\left\{-\frac{\sqrt{2}}{\pi}\frac{q^2}{\varepsilon}\left[\exp\left(-\frac{\lambda_0^2}{2q^2}\right)-\exp\left(-\frac{(\lambda_0+\varepsilon t)^2}{2q^2}\right)\right]\right\}. \tag{24}$$

In the limit $\varepsilon\to 0$, differentiating the second exponential in the overall exponent with respect to ε and setting $\varepsilon=0$ one obtains (as one should) the classical Kramers result, Eq. (3). More unexpected is the fact that in the limit $t\gg 1/\varepsilon$ this same exponential tends toward zero and one obtains

$$\lim_{t\to\infty}\delta N(t)\equiv\delta N_\infty=\delta N(0)\exp\left[-\frac{\sqrt{2}}{\pi}\frac{q^2}{\varepsilon}\exp\left(-\frac{\lambda_0^2}{2q^2}\right)\right]. \tag{25}$$

In other words, contrary to the Kramers case, equipartition (translated by $\delta N\to 0$) is not always achieved: the system may remain blocked in one of the quasiattraction basins, depending on its initial preparation.

IV. NUMERICAL EXPERIMENTS

The results reported in the preceding section will now be confronted and complemented by those of the numerical solution of the Fokker-Planck equation (18) and the stochastic simulation of the Langevin equation (16).

Figures 5(a)–5(c) depict the numerically computed prob-

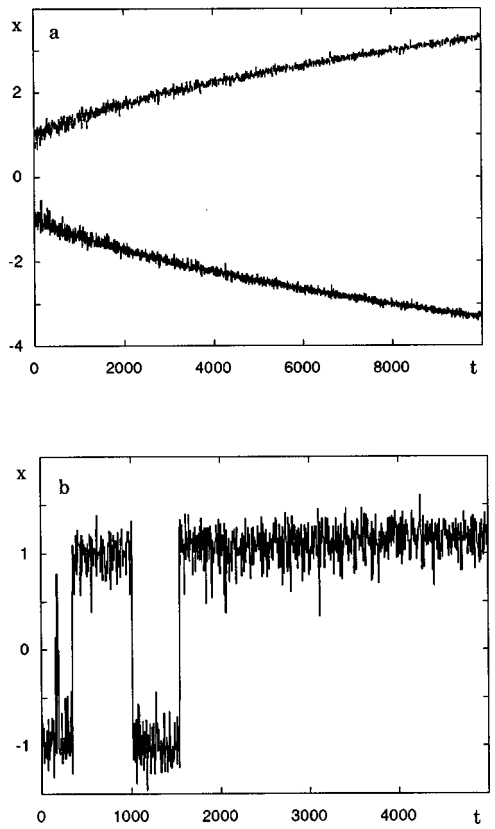

FIG. 8. Stochastic trajectory obtained numerically from Eq. (16). Parameter values $\lambda_0=1$ and $\epsilon=10^{-3}$, $q^2=0.08$ (a); $\epsilon=10^{-4}$, $q^2=0.12$ (b).

ability distribution from Eq. (18) in the limit of long times, using the method developed in Ref. [12], for $\varepsilon=10^{-4}$ and for three different values of the noise strength q^2. In addition to the equipartition result of Fig. 5(a), which according to classical Kramers theory should be the only one to prevail in the limit of long times for systems possessing a symmetric potential U around $x=0$, we observe situations where there is a marked imbalance between the probability masses in the two quasiattraction basins [Fig. 5(b)], or even an almost 100% selection of one particular basin [Fig. 5(c)]. A different view of this result, which is in full agreement with the conclusions arrived at in the preceding section, is given in Figs. 6(a)–6(c). In these figures the time evolution of the probability masses $N_+(t)$ and $N_-(t)$ inferred from the numerical solution of Eq. (18) are drawn in full and dashed lines, respectively, for the three sets of parameter values of Fig. 5. The empty circles stand for the numerically evaluated analytic result of Eq. (24) under the same conditions. The agreement is quite satisfactory, thereby establishing firmly the existence of frozen regimes in which the transitions across the barrier are quenched. These regimes are very sensitive to the parameters q^2 and ε. Indeed, the noise level q^2 necessary to achieve a certain value of δN_∞ for long times can be found from Eq. (24). It reads

$$q^2=\frac{1}{2}\,\frac{\lambda_0^2}{W\left(-\dfrac{\lambda_0^2}{\sqrt{2}\,\pi\varepsilon\,\ln\alpha}\right)}, \tag{26}$$

where $\alpha=\delta N_\infty/\delta N(0)$ and the Lambert W function $W(x)$ is defined by $W(x)\exp[W(x)]=x$. This is summarized in the ''state diagram'' of Fig. 7 with $\delta N(0)=0.5$.

In order to see how the variable $x(t)$ itself evolves in time, we perform a simulation of the Langevin equation (16). Figures 8(a) and 8(b) depict two types of *stochastic trajectory* obtained by this simulation. In Fig. 8(a), corresponding to parameter values $\lambda_0=1$, $\varepsilon=10^{-3}$, and $q^2=0.08$, we see that, starting from an initial condition in one or the other quasiattraction basins, the system remains blocked in this basin for all subsequent times, performing no transition across the barrier whatsoever. The situation is different in Fig. 8(b), corresponding to the parameter values of Fig. 5(a). Starting initially in the left quasiattraction basin, the system intermittently performs a number of transitions across the barrier before eventually getting blocked in the right quasiattraction basin. Realizations in which the blocking applies to the starting quasiattraction basin have also been observed. In addition to supporting further the conclusions based on Eqs. (24) and (25), these results are also in full agreement with the comment made in Sec. III in connection with the adiabatic approximation (20a), namely, that as time grows the system becomes increasingly localized in the immediate vicinity of one of the deterministic solutions $x_\pm(t)$.

It might seem curious at first sight that the parameter values in Fig. 8(b) correspond to the case referred to in Fig. 5(a) as ''equipartition.'' This apparent paradox is resolved by realizing that one needs to argue here in an ensemble theoretic sense: starting with N initial conditions (N large) in the left quasiattraction basin, half of the realizations generated will get settled for long times in the right basin in the equipartition case. Still, a given realization will eventually become blocked on relevant time scales, since the effective barrier will keep increasing compared to the (fixed) value of q^2, thereby bringing the system effectively to the nonequipartition regimes of Figs. 5(b)–5(c) and 6(b)–6(c). Notice that there can be no question of the equality of time and ensemble averages here, since the system is not stationary.

V. CONCLUSIONS

In this paper, the kinetics of the passage through a barrier in a bistable system undergoing a supercritical pitchfork bifurcation has been analyzed, in the presence of a ramp in the parameter controlling the bifurcation. It was shown that the ramp may considerably affect the distribution of probability mass on the two sides of the barrier. An asymptotic expression governing this distribution was derived [Eqs. (24) and (25)] and shown to be in excellent agreement with the results of simulations of the full Fokker-Planck equation associated with this system.

The possibility of practically freezing a system, upon minute changes of parameters on a preferred state by quenching at some stage, through the ramp, the transitions across the barrier provides an interesting method of control of the time evolution of multistable systems. This could be of relevance in, e.g., nonlinear optics and semiconductor physics related problems. The switching from the unstable state has been studied in great detail in such problems [5,7–9], but the long time regime associated with the passage through the barrier had so far not been addressed systematically.

A natural extension of this work is to consider bistable systems with hysteresis, as well as systems giving rise to periodic or chaotic oscillations. Another interesting situation to study pertains to the simultaneous presence of a periodic forcing and a ramp. As is well known, under a periodic forcing a noisy system is also experiencing a very different distribution of probability masses on the two sides of the barrier, associated with the phenomenon of stochastic resonance [11]. The interaction between this mechanism and the action of the ramp could open new possibilities for enhancing and controlling the sensitivity of complex systems toward environmental constraints.

ACKNOWLEDGMENT

This work was supported by the Interuniversity Attraction Poles program of the Belgian Federal Government.

[1] C. Gardiner, *Handbook of Stochastic Methods* (Springer, Berlin, 1983).
[2] See, e.g., P. Hänggi, P. Talkner, and M. Borkovec, Rev. Mod. Phys. **62**, 251 (1990).
[3] H. A. Kramers, Physica (Amsterdam) **7**, 284 (1940).
[4] G. Nicolis, *Introduction to Nonlinear Science* (Cambridge University Press, Cambridge, England, 1995).
[5] T. Erneux and P. Mandel, SIAM (Soc. Ind. Appl. Math.) J. Appl. Math. **46**, 1 (1986).
[6] G. Dewel, P. Borckmans, A. De Wit, B. Rudovics, J.-J. Perraud, E. Dulos, J. Boissonade, and P. De Kepper, Physica A **213**, 181 (1995).
[7] H. Zeglache, P. Mandel, and C. Ven den Broeck, Phys. Rev. A **40**, 286 (1989).
[8] M. Torrent and M. San Miguel, Phys. Rev. A **38**, 245 (1988).
[9] S. Belestri, M. Ciofini, R. Meucci, F. Arecchi, P. Colet, M. San Miguel, and S. Balle, Phys. Rev. A **44**, 5894 (1991).
[10] M. Suzuki, J. Stat. Phys. **16**, 477 (1977).
[11] C. Nicolis, Tellus **34**, 1 (1982).
[12] J. Chang and G. Cooper, J. Comput. Phys. **6**, 1 (1970).